

# Spinnability of Polyacrylonitrile Gel Dope in the Mixed Solvent of Dimethyl Sulfoxide/Dimethylacetamide and Characterization of the Nascent Fibers<sup>1</sup>

Liu Qun<sup>a,b,\*</sup>, Wang Yan-xiang<sup>a,b,\*\*</sup>, Niu Fang-xu<sup>a,b</sup>, Ma Lian-ru<sup>b</sup>,  
Qu Ce<sup>b</sup>, Fu Shan-long<sup>b</sup>, and Chen Mei-ling<sup>b</sup>

<sup>a</sup> Key Laboratory for Liquid–Solid Structural Evolution and Processing of Materials (Ministry of Education), Shandong University, Jinan, 250061 China

<sup>b</sup> Carbon Fiber Engineering Research Center, School of Material Science and Engineering, Shandong University, Jinan, 250061 China

\* e-mail: liuqunbabe@yahoo.com

\*\* e-mail: wyx079@sdu.edu.cn

Received March 26, 2017;

Revised Manuscript Received March 26, 2018

**Abstract**—In this work, acrylonitrile copolymers were prepared via precipitation polymerization. The copolymer solutions prepared at various ratio of dimethyl sulfoxide and dimethylacetamide were tested to prepare the nascent fibers by one-step wet-spun method. The effect of temperature, solvent ratio, molecular weight and the solid content on the rheological properties of polyacrylonitrile gel solution in different mixed solvent were studied. It was shown that the viscosity decreased with the increase of the temperature and fluctuated with the different solvent ratio reaching the minimal value at the ratio of dimethyl sulfoxide to dimethylacetamide equal to 1.25. The crystallinity of copolymers and the structure of the nascent fiber surface also depended from the solvent ratio in polymerization. The optimum conditions for spinnability of copolymers were determined. The high-quality polyacrylonitrile precursor was achieved with the controllable range of 0.5–0.8 dtex and the toughness of polyacrylonitrile precursor was greater than 6.0 cN/dtex after the wet spinning process, while the tensile strength of carbon fiber is up to 6.25 GPa after their pre-oxidation and carbonization process.

DOI: 10.1134/S0965545X18050103

## INTRODUCTION

It is well-known that the performance of polyacrylonitrile (PAN) based carbon fiber largely depends on the structure and behavior of PAN precursor [1–4]. The spinnability of PAN gel dope directly affects the behavior of precursor on its various aspects, such as surface morphology, internal density, fineness and toughness [5–7]. So, to achieve a good spinnability of PAN gel solution, a careful preparation of PAN precursor is required [8, 9]. The major factors that influence the spinnability of PAN include the spinning temperature, nature of the solvent, molecular weight of the polymer, the content of solid shear rate, the jet stretching ratio and the coagulation bath concentration [10–12]. To achieve the optimum spinnability of PAN gel solution, the mentioned factors need to be reasonable matching before starting spinning process [13, 14]. So far, the effect of the mixed solvent dimethyl sulfoxide (DMSO)/dimethylacet-

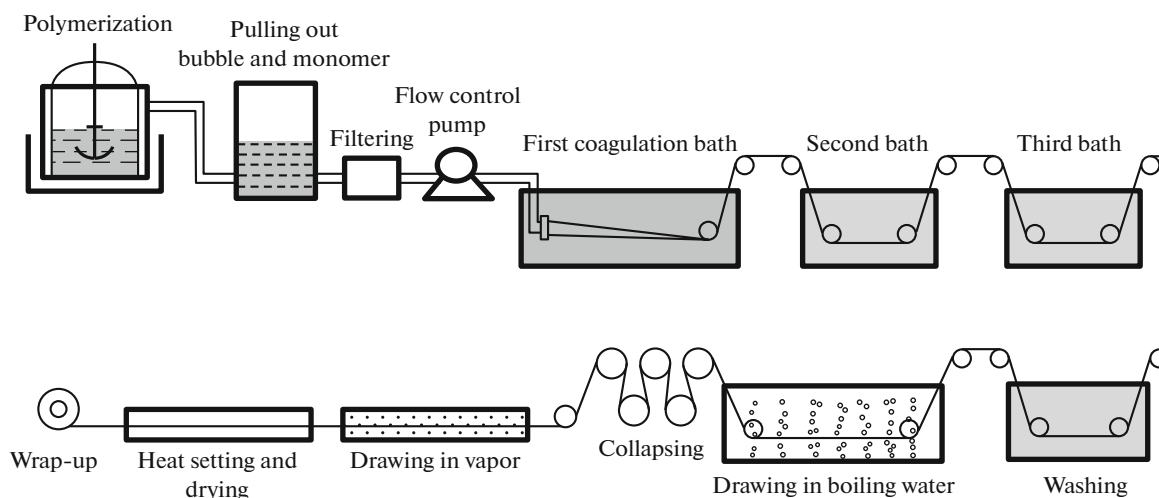
amide (DMAc) on the spinnability of PAN gel solution was often neglected and was scarcely reported. This article focuses on the rheological properties of PAN gel dope in the mixed solvent DMSO/DMAc under different conditions. The spinnability of gel solution was dramatically enhanced by the mixed solvent, which resulted in the high performance of resultant carbon fiber [1, 2].

## EXPERIMENTAL

### Materials

Acrylonitrile (AN) was purified by alkali washing followed by distillation. Itaconic acid (IA) was recrystallized twice from water. DMAc (Tianjin Fuyu Fine Chemical Co. LTD., analytical pure) and DMSO (Tianjin Chemical Reagent Co. LTD., analytical pure) were refined before dissolution.

<sup>1</sup> The article is published in the original.



Scheme 1.

### *Synthesis of Copolymer by Precipitation Copolymerization in Aqueous Medium*

Monomers AN and IA with a ratio of 99:1 (w/w) were added to the deionized water (total monomer concentration is equal to 22 wt %), then the initiator  $(\text{NH}_4)_2\text{S}_2\text{O}_8$  (0.8 wt % to the total monomers) was added and mixed homogeneously. Aqueous precipitation polymerization proceeded by stirring in  $\text{N}_2$  atmosphere at  $60^\circ\text{C}$  in a constant temperature bath. After the reaction was completed, the polymer powder was washed with the deionized water, then filtered and dried at  $60^\circ\text{C}$  for 8 h. The yield of the copolymer was 75%.

### *Preparation of PAN Gel Dope and Precursor*

The mixture of DMSO and DMAc in relative proportion was put into the conical flask. The volume solvent ratio of DMSO to DMAc was designed as 0.2, 0.5, 1.25, 2.0, 2.5 and the corresponding samples were denoted as s-x ( $x = 0.2, 0.5, 1.25, 2.0, 2.5$ ), respectively. When the mixing was completed, a certain amount of PAN powder was added into the flask and kept mixing for 6 h at  $70^\circ\text{C}$ . A series of PAN concentration including 10, 12, 14, 16, and 18 wt % were set up for the experiment. PAN gel dope can be obtained after removing bubbles by the ultrasonic treatment. Through the flow control pump, the spinning dope was sent into the first coagulation bath by the jet pipe and then washed. The preparation of PAN precursor fibers is shown in Scheme 1. PAN precursor fibers were denoted as P-x ( $x = 0.2, 0.5, 1.25, 2.0, 2.5$ )

respectively; P-DMSO and P-DMAc represent PAN fibers obtained from pure DMSO and DMAc solutions respectively.

### *Stabilization of Precursors and Carbonization of Stabilizing Fibers*

Samples were prepared by stabilizing the PAN precursor in air through different temperature zones in the order as  $190, 220, 240, 250, 260, 270, 280^\circ\text{C}$ . The stabilized fibers were carbonized in nitrogen atmosphere at a heating rate of 400 grad/min with a temperature range from  $300$  to  $800^\circ\text{C}$  and at a heating rate of 500 grad/min with a temperature range from  $800$  to  $1200^\circ\text{C}$ , up to  $1400^\circ\text{C}$  under a drawing ratio of 0.56. PAN based carbon fibers were denoted as C-x ( $x = 0.2, 0.5, 1.25, 2.0, 2.5$ ), respectively.

### *Characterization Techniques*

Brookfield DV-II + ProCone/Plate rotating viscometer was used for viscosity test and the testing temperature was varied from  $50$  to  $80^\circ\text{C}$ . The morphology and microstructure of the obtained samples were investigated by a field emission scanning electron microscope (SEM, JSM-6701F). Further detailed structure study of the nascent fiber was carried out by a high resolution transmission electron microscopes (HRTEM, EOL, JEM-2100) operated at 200 kV. Crystallite structures were determined by XRD (Phillips PW1710 X-ray diffractometer) using  $\text{CuK}_\alpha$  radiation from  $5^\circ$  to  $50^\circ$ . The fibers were cut into pieces and ground into powder after the freeze-drying, then the infrared absorption spectrum was obtained by the highly pure potassium bromide tableting (Thermo Nicolet Avatar 370FTIR spectrophotometer). To assess the variation of tensile strength of fibers for each process, the single-fiber

tensile test was performed with a gauge length of 20 mm and a crosshead speed of 2 mm/min by a XQ-1 tensile tester from Donghua University. Total mass of polymerization system before reaction is  $m_1$ , the total monomer concentration is  $c_1$ , and the mass of the dried copolymer is  $m_2$ .

## RESULTS AND DISCUSSION

### *Effect of Different Conditions on PAN Gel Dope Viscosity*

DMSO, dimethylformamide (DMF) or DMAc are commonly for the preparation of PAN gel dope [15–17]. PAN/DMSO solution has a good stability but poor fluidity and it has a higher viscosity when compared with DMF/DMSO and DMAc/DMSO under the same conditions. Effect of the solvent ratio on PAN gel dope at solid content 16% from 50 to 80°C for PAN copolymer with the number average molecular weight is  $3 \times 10^5$  is shown in Fig. 1. As is seen, with the increase of the ratio (DMSO/DMAc), the apparent viscosity of PAN gel dope increases and the viscosity reaches the maximum when the ratio is 1 : 1, and then sharply drops down, after that it rises steadily [18]. From Fig. 1, a relatively small value appears when the solvent ratio is 1.25 : 1.00 and then rises steadily. This result can be explained through the principles of solubility with similar conditions. The solubility parameter of the resulted mixed solvents  $\delta_m$  can be calculated:  $\delta_m = \delta_{\text{DMSO}}\phi_{\text{DMSO}} + \delta_{\text{DMAc}}\phi_{\text{DMAc}}$ , where  $\delta_{\text{DMSO}}$ ,  $\delta_{\text{DMAc}}$  are the solubility parameters of DMSO and DMAc, respectively;  $\phi_{\text{DMSO}}$ ,  $\phi_{\text{DMAc}}$  are the volume fraction of DMSO and DMAc.

It is known that the solubility parameters of PAN, DMSO, DMAc are 26.0, 27.4, and 22.7 (J/cm<sup>3</sup>)<sup>1/2</sup> respectively. In our research, ratio of monomers AN/IA is 99/1, and we believe that IA does not affect solubility parameters. So we can get  $\delta_m = 26.0$  (J/cm<sup>3</sup>)<sup>1/2</sup> when DMSO : DMAc = 1.83. As the polar polymer, PAN can be dissolved in DMSO, DMAc and other polar solvents with a similar solubility parameter.

The following consideration may be provided. It is found that the viscosity of gel dope prepared by PAN/DMSO is higher than that by PAN/DMAc in the same conditions, which means that DMSO plays a more important role in the viscosity. This calculation means the ratio of DMSO : DMAc located at 1.83 is the best. However in fact, the viscosity of the PAN gel dope is not the lowest when the solvent ratio is 1.83 (Fig. 1). Parameters of solubility have certain deviation comparing the spinning experiment in the lab. According to the above mentioned, the viscosity is relatively higher when the ratio DMSO : DMAc = 1.83, which reduces spinnability of the solution. This is because the proportion of DMSO is quite high and

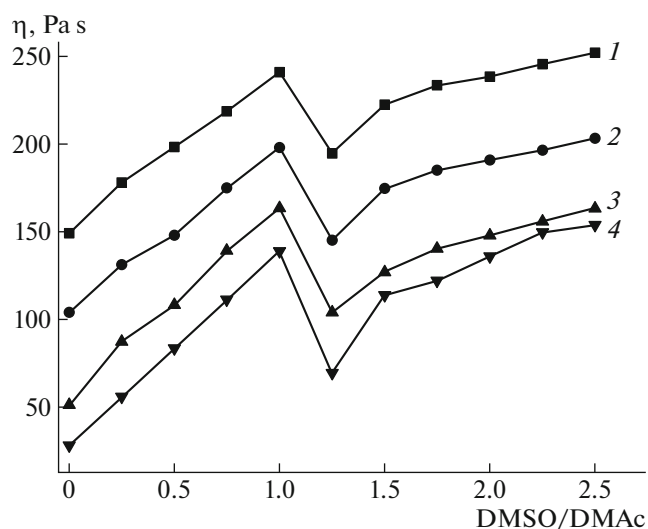
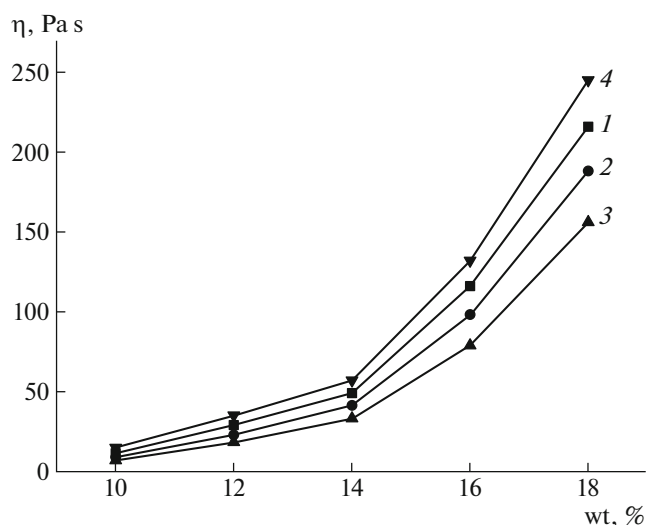


Fig. 1. The apparent viscosity of PAN gel solution at different solvent ratio at  $T = (1)$  50,  $(2)$  60,  $(3)$  70, and  $(4)$  80°C.

DMSO proportion influences the viscosity of the PAN gel dope more. The minimum viscosity of gel dope appears when the ratio DMSO : DMAc = 1.25 where DMSO proportion is not high. The solubility parameter of mixed solvents in the corresponding area doesn't have much difference from PAN and the mixed solvents can dissolve PAN well.

Keeping the other conditions constant, the molecular weight of  $3 \times 10^5$  and the solvent ratio of 1.25 : 1.00, effect of solid content on the PAN gel dope is shown in Fig. 2. With the increase of solid content, the viscosity of PAN gel dope increases slowly before the point of 14% and considerably increases after 14%, which is due to achieving crossover concentration. The molecular chain spacing obviously decreases when the solid content exceeds the critical value. So, as the quantity of PAN molecular chains increases in the solution, the molecular chains are expected to collide more rapidly and chain segment motion needs to overcome more resistance. The above kind of phenomenon becomes more obvious with the increase of the solid content, ultimately, which leads to the sharply-increasing viscosity of the solution at the macro level. When the solid contents of PAN are further increased after 14%, a sharp increase in the viscosity of dope gel is observed. However the viscosity of spinning dope at 14% solid contents is lower than required for spinning. After doing many experiments in the lab, it was been verified that the solid content around 16% was the moderate viscosity for spinning, the gel dope with the proper content would be easy to be spun and the nascent fiber will not be broken in the spinning process.



**Fig. 2.** The apparent viscosity of PAN gel solution at different solid content at  $T = (1) 50, (2) 60, (3) 70,$  and  $(4) 80^\circ\text{C}$ .

To discuss the relationship between the temperature and the apparent viscosity in detail, the curves of PAN gel solution at different temperature are described in Fig. 3, as the ratio of DMSO/DMAC is 0.2 : 1.0, 0.5 : 1.0, 1.25 : 1.00, 2.0 : 1.0 to 2.5 : 1.0 while the solid content is kept at 16%. As shown in Fig. 3, when the temperature rises, the apparent viscosity decreases and the downward trend remains unaffected by the change in the proportions of solvents, which is mainly because the flowing unit of PAN solution is the mobile chain section rather than the entire moving polymer [19, 20]. The high temperature will lead to the increase of the chain-spacing of PAN, and at the same time decreases the interaction force between molecules which also contributes to the decrease of the viscosity of PAN [21, 22], so the spinning temperature was set between 60 and 70°C.

**Table 1.** Parameters for WAXRD curves of PAN polymers in Fig. 4

Sample	Solvent ratio	$2\theta$ , deg	FWHM, deg	$d$ , nm	$L_c$ , nm	CI, %
1	2.5 : 1.0	17.2	1.1	0.5	5.2	54
2	2.0 : 1.0	17.2	1.6	0.5	4.0	52
3	1.25 : 1.00	17.2	1.8	0.5	4.0	48
4	0.5 : 1.0	17.2	1.8	0.5	4.2	48
5	0.2 : 1.0	17.2	2.3	0.5	4.5	48

$2\theta$ —Bragg diffraction angle; FWHM—the full width at half maximum;  $d$ —interplanar spacing;  $L_c$ —crystalline size; CI—crystallinity.

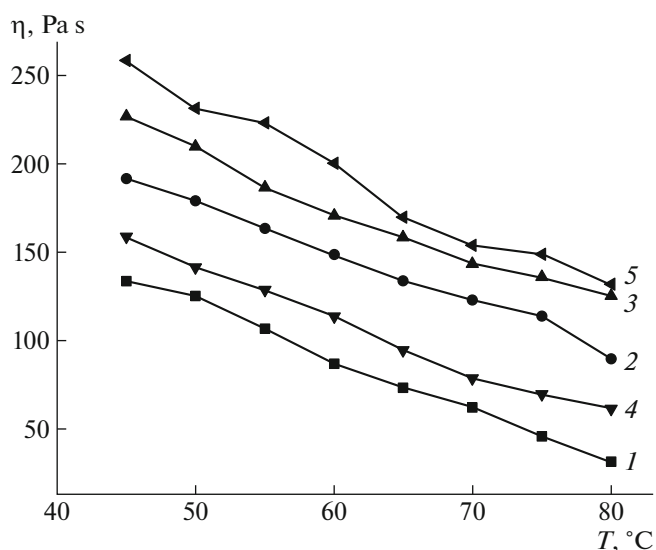


**Fig. 3.** The apparent viscosity of PAN gel solution at different temperature at different solvent ratio of DMSO/DMAC: (1) s-0.2, (2) s-0.5, (3) s-1.25, (4) s-2.0, (5) s-2.5.

It could be found that the crystal structure change can be characterized when different solvents in the preparation process of the gel dope are chosen through measuring the crystallinity of PAN. In some sense, the disordered PAN molecular chains become orientated after the drawing-process [23]. The random orientation of PAN has a certain degree of crystallinity, which has a great influence on the nascent fiber, and the rigidity of nascent filaments would be larger with the higher crystallinity. It should be noticed that defects could be caused by further stretching which will reduce the strength of the precursor. In contrast, the molecular chains with the lower crystallinity are easy to flow in stretching process and the molecular chains stretch along the stress direction. PAN precursors acquire the higher strength and smaller grain size after further stretching. The XRD spectrum for the finally obtained PAN fiber at the different solvent ratio is shown in Fig. 4. It is clear from XRD spectrum that the diffraction peak (100) near  $17^\circ$  is more obvious, and the diffraction peak (110) near  $29^\circ$  is almost covered by some amorphous diffuse peaks.

From the data in Table 1, the crystallinity of PAN decreases after dissolution because the solvent destroys the area of crystallization of PAN. The crystallization peak changes a little and the full width at half maximum is enhanced as the content of DMSO reduces, which implies that the decrease in the proportion of DMSO has an unfavorable influence that is to reduce the crystalline region of polymer on the crystallinity of polymer. The crystallinity and grain size under the solvent ratio at 1.25 : 1.00 is reduced by

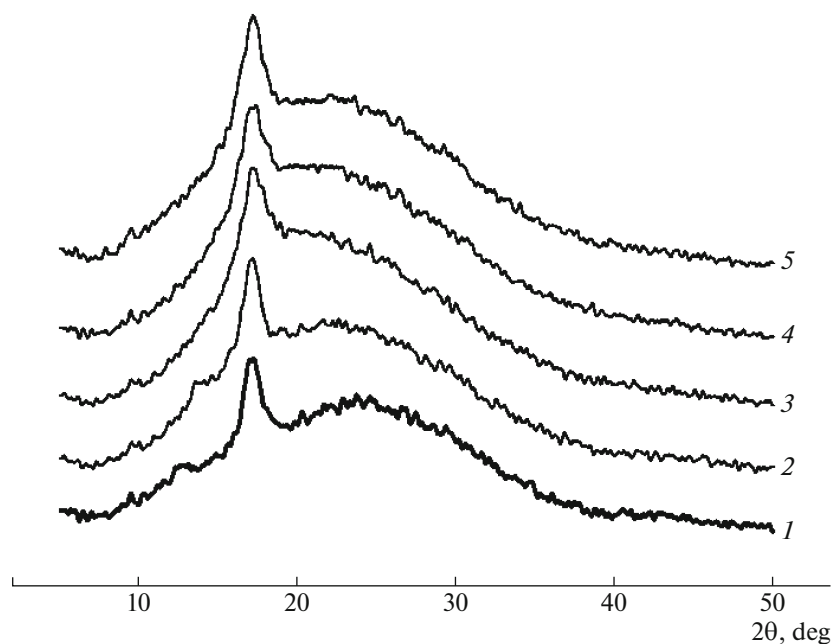


**Fig. 4.** XRD curves of the attained PAN polymers at different solvent ratio of DMSO/DMAc: (1) s-0.2, (2) s-0.5, (3) s-1.25, (4) s-2.0, (5) s-2.5.

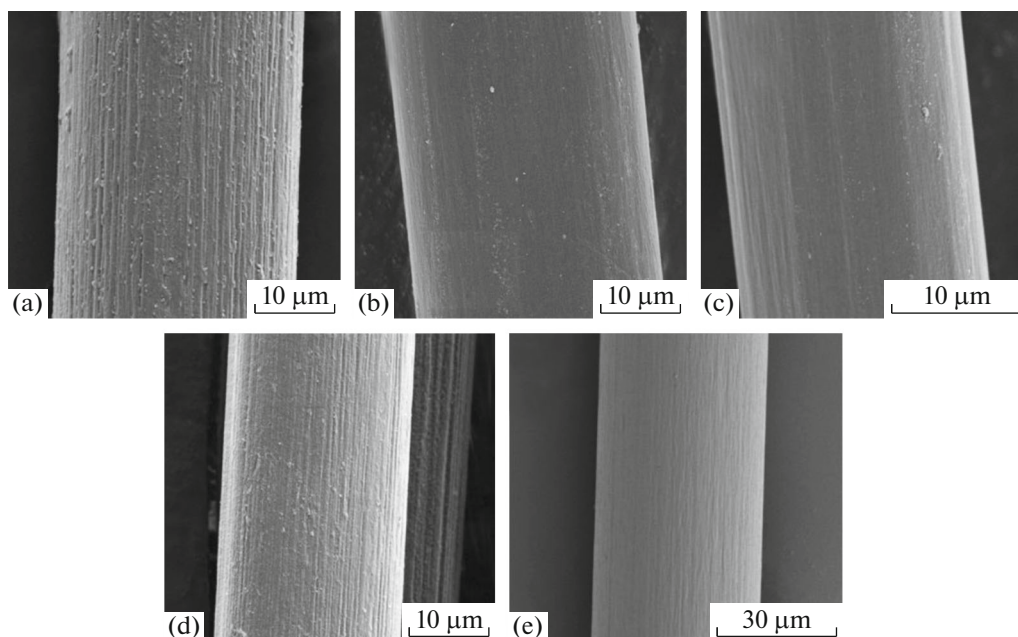
10% as compared with that under the solvent ratio of 0.2 : 1.0. Therefore, in order to enhance the crystallization of polymer, the solvent ratio of 1.25 : 1.00 is favored for DMSO/DMAc.

Figure 5 reflects the surface morphology of PAN nascent fibers produced from the different volume ratio of DMSO/DMAc by the wet spinning technique. The orderly-arranged groove structure can be observed along the axial surface of PAN fibers obtained using different ratios of DMSO/DMAc. Groove structure was produced when the solidification occurred in coagulation bath and remained on the surface of the fiber all the time. The generation of surface grooves is a reflection of complex factors during the fiber solidification process. As the spinneret is immersed under the surface of liquid in coagulation bath, the swelling effect of gel dope occurred after its extrusion, the instantaneous phase separation occurred and the double diffusion was made between coagulation bath and the nascent fibers simultaneously. Two phases including polymer phase and organic-aqueous solution phase can co-exist and the swelling gel fiber state was gradually formed. The groove structures are deep and the thickness is not uniform as seen in Fig. 5a. The groove structures became more homogeneous and the orientation degree also improved. The depth of grooves became shallow gradually which implied its orientation degree of groove structure was improved. The thickness and depth of groove structure became uniform, as shown in Figs. 5b and 5c. In addition, the radial dimension of groove became thinner. The aggregation of macromo-

lecular chains along the fiber axis led to the orientation. PAN fiber was affected by the drafting force, which formed some relatively complete dense microfibrils and fibril structure. Changes of groove morphology were partly macro-external embodiment of changing internal microstructure because PAN dope had not been fully solidified in the first coagulation bath, and its gel network structure was easily damaged and prone to be destroyed under the drafting force. The nascent fibers generally had a larger diameter size because of the negative drafting force in the spinning process. As shown in Figs. 5d and 5e, the die-swell effect has largely disappeared in the s-0.5 and s-0.2 fibers under the joint action of drafting force and internal stress. The die-swell effect and the volume shrinkage effect caused by double diffusion and phase separation occurred quickly, so the surface of fiber became deep, the diameter of fiber reduced gradually under the action of multistage drafting and densification, the crystallinity and compactness were reduced substantially.

Images of the nascent fiber produced by the wet spinning technique keeping the volume ratio of DMSO/DMAc at 1.25 : 1.00 are shown in Fig. 6. As it seen, it had the longitudinal section slice with the thickness of 50 and 100 nm. There are many folds on the slice cross section and the ultra-thin section is in  $\sim 20\text{--}30\ \mu\text{m}$  length along the radial direction but it is not the diameter of nascent fiber. Many scale-like layered structures of the nascent fiber can be seen in Fig. 6a1 due to the vertically-downward cutting, the dense cortex is 500 nm thick where plenty of carbon





**Fig. 5.** SEM images of PAN nascent fibers at the different volume ratio of DMSO/DMAc: (a) s-2.5; (b) s-2; (c) s-1.25; (d) s-0.5; (e) s-0.2 by wet spinning stages.

atoms gather in as shown in Fig. 6a1. Lamellae are about 50 nm thick and have the uneven length. The intermediate part of nascent fiber was chopped due to the inhomogeneous slicing. As shown in Fig. 6b, the nascent fiber micro structure with small thickness can be found in the edge of pieces, but the layered structure is not obvious because of the thin slices as shown in Fig. 6b1. This is because that polymer chain performing connection function can be seen along axial direction in fiber and these amorphous polymers con-

nect the layered structure of nascent fiber. The length of slice is about  $\sim 20\text{--}25\ \mu\text{m}$  in the radial direction, as shown in Fig. 6c. The slice structure of nascent fiber is very similar when compared with Figs. 6a1 and 6c1, and the distribution of scale-like structure is uniform. The overall structure of the fiber is amorphous, and the lamellar structure has low crystallinity.

IR spectra of PAN polymers obtained at different volume ratio of DMSO/DMAc are shown in Fig. 7. The bands located at  $\sim 1450\text{--}1430$ ,  $\sim 1360\text{--}1340$ , and  $\sim 1280\text{--}1230\ \text{cm}^{-1}$  are assigned to the C–H vibrations of different modes. The absorption bands at 1250 and  $1230\ \text{cm}^{-1}$  are stereospecific due to the wagging mode of the methine (–CH) group coupled with the rocking mode of methylene (–CH<sub>2</sub>) group. The bands at 1660 and  $1638\ \text{cm}^{-1}$  are overlapped with the carbonyl stretching band of acid groups at  $\sim 1735\text{--}1737\ \text{cm}^{-1}$  due to hydrogen bonding. The strong band in the range of  $\sim 1750\text{--}1700\ \text{cm}^{-1}$  exists in the copolymers due to the C=O stretching. The broad band in the range  $\sim 2600\text{--}3200\ \text{cm}^{-1}$  is assigned to C–H stretching in –CH, MCH<sub>2</sub>, –CH<sub>3</sub>. The position of the C≡N absorption band at  $2240\ \text{cm}^{-1}$ , which is the strongest absorption band in the polymers, indicates the presence of uninterrupted long sequences for the AN units in polymers. The broad band in the range  $\sim 3200\text{--}3600\ \text{cm}^{-1}$  is attributed to the O–H stretching. Evidently, that all the spectra are identical as the volume ratios of DMSO/DMAc do not affect the chemical composition of PAN polymers.

**Table 2.** The performance of precursors (temperature 60 to 70°C, the solid contents 1%)

Sample	<i>D</i> , dtex	BF, cN	Tenacity, cN/dtex	Ext, %
P-DMSO	0.69	4.1	5.9	9.1
P-2.5	0.65	3.9	6.0	9.5
P-2	0.67	4.2	6.3	10.1
P-1.25	0.56	4.6	8.2	10.3
P-0.5	0.66	4.5	6.8	9.5
P-0.2	0.72	4.7	6.5	10.1
P-DMAc	0.71	4.4	6.2	9.9

*D*—denier of the fiber; BF—brute force; Ext—elongation at break. Every sample was tested 40 times to measure BF and *D* of single fiber to acquire average value.

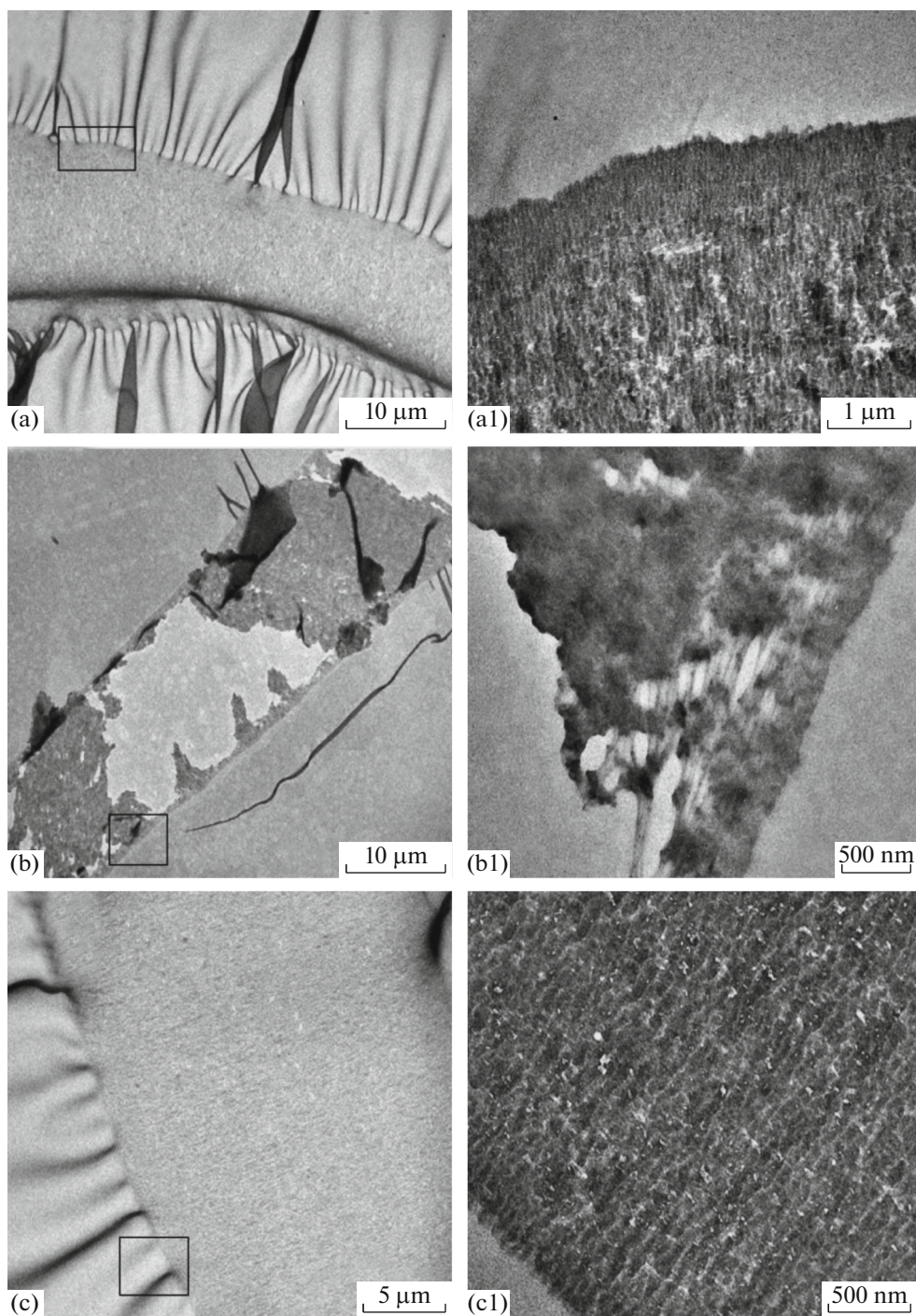


**Fig. 6.** TEM images of ultrathin longitudinal section of PAN nascent fiber with different thickness. (a1), (b1), (c1) are parts larger images of (a), (b), (c) respectively.

The mechanical properties recorded in Tables 2 and 3 are measured for precursors and carbon fibers that are produced by keeping the spinning temperature between 60 and 70°C and the solid content solid content of PAN gel dope at 16%. The tenacity  $T$  can be calculated:

$$T = \frac{BF}{D}$$

As shown in Table 2, the tenacity of precursors increased as DMSO content decreased, but when DMSO content dropped to some extent, the value of tenacity began to reduce. The tenacity of precursors

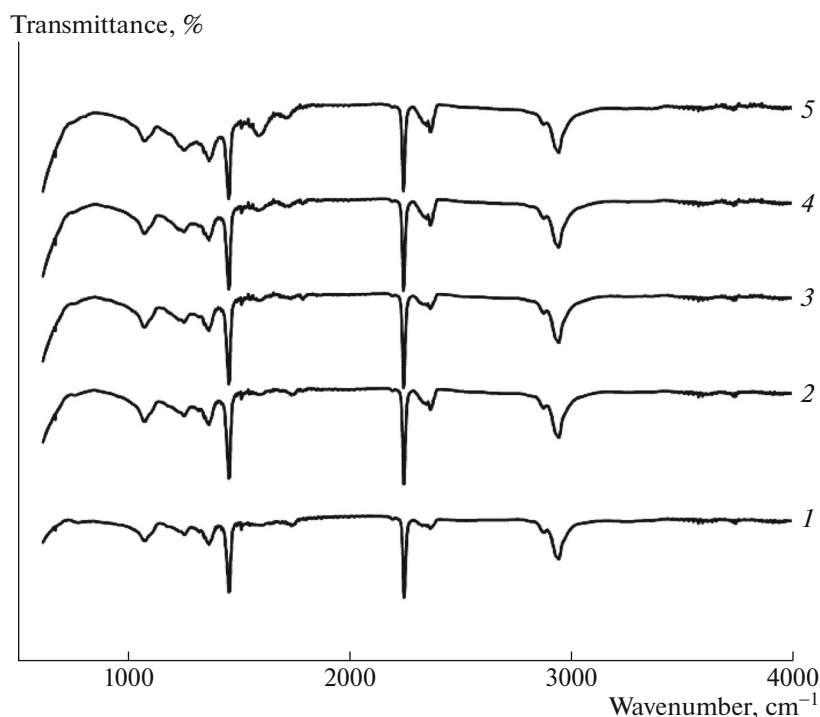


Fig. 7. The infrared spectrum of the polymers: (1) s-0.2, (2) s-0.5, (3) s-1.25, (4) s-2.0, (5) s-2.5.

varied from 5.94 to 8.21 cN/dtex and then dropped to 6.19 cN/dtex with the decreasing of DMSO. It was obtained as high as 8.21 cN/dtex when DMSO/DMAc was 1.25. After preoxidation and carbonization process, it can be found from Table 3 that the tensile strength rose up from 6.12 to 6.52 GPa and then dropped to 5.91 GPa with the increasing of DMSO corresponding to Table 2. In other words, the corresponding tensile strength of resultant carbon fiber increased at first and then decreased faster as increasing the DMSO content. The corresponding tensile strength of resultant carbon fiber could reach 6.52 GPa when DMSO/DMAc was 1.25.

## CONCLUSIONS

The solid content has an important effect on the rheological behavior of PAN gel dope. Solution viscosity increases slowly before the critical point, however this increase is radical after a tipping point. The proportion of solvent viscosity of PAN gel dope has a significant effect on PAN crystallization. When the volume ratio of DMSO/DMAc is 1.25 : 1.00, the solution viscosity is the minimum and PAN crystallization is better, so the spinnability of PAN gel dope is optimal. The optimum spinnability of PAN gel solution is: the spinning-temperature lies in the range of 60–70°C, the solvent ratio is 1.25 : 1.00 and the solid con-

Table 3. The performance of carbon fibers

Sample	Tensile force, N	Tensile strength, GPa	Tensile modulus, GPa	Ext, %
C-DMSO	1620	6.1	220	1.8
C-2.5	1650	6.2	240	1.9
C-2	1650	6.2	240	1.9
C-1.25	1730	6.5	280	2.2
C-0.5	1590	6.0	230	2.1
C-0.2	1580	6.0	240	1.9
C-DMAc	1570	5.9	240	1.9

Every sample was tested 40 times to measure tensile strength of single fiber to acquire average value.



tent is 16%. The gel dope was prepared and spun in the coagulation where the volume ratio of DMSO/DMAc was 1.25 for the mixed solvent. The overall structure of nascent fiber is amorphous, and its lamellae has the uneven length and low crystallinity. After the spinning progress, the tenacity of precursors can be 8.21 cN/dtex and the corresponding tensile strength of carbon fiber could achieve 6.52 GPa after its preoxidation and carbonization process.

#### ACKNOWLEDGMENTS

This work was supported by the Natural Science Foundation in Shandong Province (ZR2017MEM011), IIFSDU (2016JC004) and National Natural Science Foundation of China (51773110, 51573087).

#### REFERENCES

1. J. Kaur, K. Millington, and S. Smith, *J. Appl. Polym. Sci.* **133** (38), 43963 (2016).
2. S. B. Hanna, A. A. Yehia, M. N. Ismail, and A. I. Khalaf, *J. Appl. Polym. Sci.* **123** (4), 2074 (2012).
3. M. Kirsten, J. Meinl, K. Schonfeld, A. Michaelis, and C. Cherif, *J. Appl. Polym. Sci.* **133** (29), 43698 (2016).
4. H. G. Chae, B. A. Newcomb, P. V. Gulgunje, Y. D. Liu, K. K. Gupta, M. G. Kamath, and S. Kumar, *Carbon* **93**, 81 (2015).
5. M. Wang, Y. Xiao, W. Cao, N. Jiao, W. Chen, and L. H. Xu, *Polym. Adv. Technol.* **26** (2), 136 (2015).
6. L. Tan, J. Pan, and A. Wan, *Colloid Polym. Sci.* **290** (4), 289 (2012).
7. X. Liu, C. Zhu, H. Dong, B. Wang, R. Liu, N. Zhao, R. Liu, and J. Xu, *Colloid Polym. Sci.* **293** (2), 587 (2015).
8. Z. Zhou, X. Wang, S. Faraji, D. B. Philip, Q. W. Li, and Y. Zhu, *Carbon* **75**, 307 (2014).
9. A. Ju, S. Guang, and H. Xu, *Chin. Chem. Lett.* **23** (11), 1307 (2012).
10. X. Y. Qin, Y. G. Lu, H. Xiao, Y. C. Hao, and P. Ding, *Carbon* **49** (13), 4598 (2011).
11. S. Liu, H. Jiang, W. Du, and D. Pan, *Fibers Polym.* **13** (7), 846 (2012).
12. N. Byrne, L. Alexis, and F. Bronwyn, *J. Mater. Chem. A* **2** (10), 3424 (2014).
13. R. Dong, M. Keuser, X. Zeng, J. Zhao, Y. Zhang, C. Wu, and D. Pan, *J. Polym. Sci., Part B: Polym. Phys.* **46** (19), 1997 (2008).
14. R. Devasia, C. P. Nair, and K. N. Ninan, *Polym. Adv. Technol.* **19** (12), 1771 (2008).
15. A. F. Ismail, M. A. Rahman, A. Mustafa, and T. Matsuura, *Mater. Sci. Eng., A* **485** (1), 251 (2008).
16. E. A. Morris, M. C. Weisenberger, and G. W. Rice, *Fibers* **3** (4), 560 (2015).
17. Y. Eom and B. C. Kim, *Polymer* **55** (10), 2570 (2014).
18. J. Hao, F. An, Y. X. Yu, P. C. Zhou, Y. D. Liu, and C. X. Lu, *J. Appl. Polym. Sci.* **134** (5), 44390 (2016).
19. J. S. Tsai and C. H. Lin, *J. Appl. Polym. Sci.* **42** (11), 3045 (1991).
20. T. Y. Wang, H. C. Chang, Y. T. Chiu, and J. L. Tsai, *J. Appl. Polym. Sci.* **132** (2), 41265 (2015).
21. L. Tan, H. Chen, D. Pan, and N. Pan, *Eur. Polym. J.* **45** (5), 1617 (2009).
22. A. Ju, S. Guang, and H. Xu, *Carbon* **54**, 323 (2013).
23. N. Yusof and A. F. Ismail, *J. Anal. Appl. Pyrolysis* **93**, 1 (2012).